

G.E. Volovik

Twenty years of magnon Bose condensation and spin current superfluidity in $^3\text{He-B}$

02.04.2008

Keywords superfluid ^3He , spin-current superfluidity, magnon Bose-Einstein condensation

Abstract 20 years ago a new quantum state of matter was discovered and identified^{1,2,3,4,5,6,7}. The observed dynamic quantum state of spin precession in superfluid $^3\text{He-B}$ bears the properties of spin current superfluidity, Bose condensation of spin waves – magnons, off-diagonal long-range order and related phenomena of quantum coherence.

PACS numbers: 67.30.er; 75.30.Ds; 67.10.Ba

1 Introduction

Nature knows different types of ordered states.

One major class is represented by equilibrium macroscopic ordered states exhibiting spontaneous breaking of symmetry. This class contains crystals; nematic, cholesteric and other liquid crystals; different types of ordered magnets (antiferromagnets, ferromagnets, etc.); superfluids, superconductors and Bose condensates; all types of Higgs fields in high energy physics; etc. The important subclasses of this class contain systems with macroscopic quantum coherence exhibiting off-diagonal long-range order (ODLRO), and/or nondissipative superfluid currents (mass current, spin current, electric current, hypercharge current, etc.). The class of ordered systems is characterized by rigidity, stable gradients of order parameter (non-dissipative currents in quantum coherent systems), and topologically stable defects (vortices, solitons, cosmic strings, monopoles, etc.).

Low Temperature Laboratory, Helsinki University of Technology, P.O.Box 5100, FIN-02015 HUT, Finland, and L.D. Landau Institute for Theoretical Physics, 119334 Moscow, Russia
Tel.: 358-9-4512963
Fax: 358-9-4512969
E-mail: volovik@boojum.hut.fi

A second large class is presented by dynamical systems out of equilibrium. Ordered states may emerge under external flux of energy. Examples are the coherent emission from lasers; water flow in a draining bathtub; pattern formation in dissipative systems; etc.

Some of the latter dynamic systems can be close to stationary equilibrium systems of the first class. For example, ultra-cold gases in optical traps are not fully equilibrium states since the number of atoms in the trap is not conserved, and thus the steady state requires pumping. However, if the decay is small then the system is close to an equilibrium Bose condensate, and experiences all the corresponding superfluid properties. Bose condensation of quasiparticles whose number is not conserved is a timely topic in present literature: this is Bose condensation of magnons, rotons, phonons, polaritons, excitons, etc.

There are two different schools in the study of the Bose condensation of quasiparticles. In one of them, Bose condensation (and ODLRO) of quasiparticles is used for describing an equilibrium state with diagonal long-range order, such as crystals, and magnets (see^{8,9} and references therein). This is somewhat contradictory, since the essentially non-equilibrium phenomenon of condensation of the non-conserved quasiparticles cannot be used for the description of a true equilibrium state (see e.g.¹⁰). Actually Bose condensation here serves as the instrument for the description of the initial stage of the soft instability which leads to symmetry breaking and formation of the true equilibrium ordered state of the first class. For example, using the language of Bose condensation of phonons one can describe the soft mechanism of formation of solid crystals¹¹. In the same way Bose condensation of magnons can be used for the description of the soft mechanism of formation of ferromagnetic and antiferromagnetic states (see e.g.¹²). The growth of a single mode in the non-linear process after a hydrodynamic instability¹³ can be also discussed in terms of the ‘Bose condensation’ of the classical sound or surface waves¹⁴.

A second school considers Bose condensation of quasiparticles as a phenomenon of second class, when the emerging steady state of the system is not in a full thermodynamic equilibrium, but is supported by pumping of energy, spin, atoms, etc. The distribution of quasiparticles in these dynamic states is close to the thermodynamic equilibrium with a finite chemical potential which follows from the quasi-conservation of number of quasiparticles. In this way, recent experiments in Refs.¹⁵ and¹⁶ may be treated as Bose condensation of magnons and exciton polaritons, respectively (see also Ref.¹⁷ and Appendix G; the possibility of the BEC of quasiequilibrium magnons has been discussed in Ref.¹⁸). The coherence of these dynamical states is under investigation¹⁹.

But not everybody knows that the coherent spin precession discovered in superfluid ³He more than 20 years ago, and known as Homogeneously Precessing Domain (HPD), is the true Bose-Einstein condensate of magnons (see e.g. reviews^{20,21}). This spontaneously emerging steady state preserves the phase coherence across the whole sample. Moreover, it is very close to the thermodynamic equilibrium of the magnon Bose condensate and thus exhibits all the superfluid properties which follow from the off-diagonal long-range order (ODLRO) for magnons.

In the absence of energy pumping this HPD state slowly decays, but during the decay the system remains in the state of the Bose condensate: the volume of

the Bose condensate (the volume of HPD) gradually decreases with time without violation of the observed properties of the spin-superfluid phase-coherent state. A steady state of phase-coherent precession can be supported by pumping. But the pumping need not be coherent – it can be chaotic: the system chooses its own (eigen) frequency of coherent precession, which emphasizes the spontaneous emergence of coherence from chaos.

2 HPD – magnon Bose condensate

2.1 Larmor precession

The crucial property of the Homogeneously Precessing Domain is that the Larmor precession spontaneously acquires a coherent phase throughout the whole sample even in an inhomogeneous external magnetic field. This is equivalent to the appearance of a coherent superfluid Bose condensate. It appears that the analogy is exact: HPD is the Bose-condensate of magnons.

The precession of magnetization (spin) occurs after the magnetization is deflected by an angle β by the rf field from its equilibrium value $\mathbf{S} = \chi\mathbf{H}$ (where $\mathbf{H} = H\hat{z}$ is an external magnetic field and χ is spin susceptibility of liquid ^3He):

$$S_x + iS_y = S_{\perp} e^{i\omega t + i\alpha} , \quad (1)$$

$$S_{\perp} = \chi H \sin \beta , \quad S_z = \chi H \cos \beta . \quad (2)$$

The immediate analogy²² says that in precession the role of the number density of magnons is played by the deviation of the spin projection S_z from its equilibrium value:

$$n_M = \frac{S - S_z}{\hbar} = \frac{S(1 - \cos \beta)}{\hbar} . \quad (3)$$

The number of magnons is a conserved quantity if one neglects the spin-orbit interaction. It is more convenient to work in the frame rotating with the frequency ω of the rf field, where the spin is stationary if relaxation is neglected. The free energy in this frame is

$$F(\beta) = (\omega - \omega_L)S_z + E_{so}(\beta) . \quad (4)$$

Here $\omega_L = \gamma H$ is the Larmor frequency; γ is the gyromagnetic ratio of the ^3He atom. The precession frequency plays the role of the chemical potential μ for magnons:

$$\mu = \omega ; \quad (5)$$

while the local Larmor frequency $\omega_L(\mathbf{r})$ plays the role of external potential; and $E_{so}(\beta)$ is the energy of spin-orbit interaction. The properties of the precession depend on $E_{so}(\beta)$: stable precession occurs when $E_{so}(\beta)$ is a concave function of $\cos \beta$. This is what occurs in $^3\text{He-B}$ (see Appendix A).

2.2 Spectrum of magnons: anisotropic mass

The important property of the Bose condensation of magnons in $^3\text{He-B}$ is that the mass of magnons is anisotropic, i.e. it depends on the direction of propagation (see Appendix B). The spectrum of magnons (transverse spin waves) is

$$\omega(\mathbf{k}) = \omega_L + \frac{\hbar k_z^2}{2m_M^\parallel(\beta)} + \frac{\hbar k_\perp^2}{2m_M^\perp(\beta)}, \quad (6)$$

where the longitudinal and transverse masses depend on the tilting angle. Both masses are much smaller than the mass m of the ^3He atom:

$$\frac{m_M}{m} \sim \frac{\hbar\omega_L}{E_F}, \quad (7)$$

where $E_F \sim 1K$ is the Fermi energy in ^3He liquid (see Appendix B). In the co-rotating frame the spectrum is shifted

$$\omega_{\text{co-rot}}(\mathbf{k}) = \omega_L - \omega + \frac{\hbar k_z^2}{2m_M^\parallel(\beta)} + \frac{\hbar k_\perp^2}{2m_M^\perp(\beta)}, \quad (8)$$

which corresponds to the chemical potential $\mu = \omega$.

2.3 Bose condensation of magnons

The value $\mu = \omega_L$ is critical: when μ crosses the minimum of the magnon spectrum, the Bose condensation of magnons with $k = 0$ occurs resulting in the phase-coherent precession of spins and spin superfluidity at $\mu > \omega_L$. In $^3\text{He-B}$, the Bose condensate of magnons is almost equilibrium. Though the number density of magnons in precessing state is much smaller than the density number n of ^3He atoms

$$\frac{n_M}{n} \sim (1 - \cos\beta) \left(\frac{\hbar\omega_L}{E_F} \right), \quad (9)$$

their mass is also by the same factor smaller (see Eq.(7)). The critical temperature of the Bose condensation of magnons, which follows from this mass is

$$T_{\text{BEC1}} \sim \frac{\hbar^2 n_M^{2/3}}{m_M} \sim \frac{E_F^{4/3}}{(\hbar\omega_L)^{1/3}} \sim 10E_F. \quad (10)$$

The more detailed calculations gives even higher transition temperature (see Appendix C). In any case the typical temperature of superfluid ^3He of order $T \sim 10^{-3}E_F$ is much smaller than the condensation temperature, and thus the Bose condensation is complete.

2.4 ODLRO of magnons

In terms of magnon condensation, the precession can be viewed as the off-diagonal long-range order (ODLRO) for magnons. The ODLRO is obtained using the Holstein-Primakoff transformation

$$\begin{aligned}\hat{b}\sqrt{1-\frac{b^\dagger b}{2S}} &= \frac{\hat{S}_+}{\sqrt{2S\hbar}}, \\ \hat{b}^\dagger\sqrt{1-\frac{b^\dagger b}{2S}} &= \frac{\hat{S}_-}{\sqrt{2S\hbar}}, \\ \hat{b}^\dagger\hat{b} &= \frac{S-S_z}{\hbar}.\end{aligned}\quad (11)$$

In the precessing state of Eq.(1), the operator of magnon annihilation has a non-zero vacuum expectation value – the order parameter:

$$\Psi = \langle \hat{b} \rangle = \sqrt{\frac{2S}{\hbar}} \sin \frac{\beta}{2} e^{i\omega t + i\alpha}. \quad (12)$$

So, $\sin(\beta/2)$ plays the role of the modulus of the order parameter; the phase of precession α plays the role of the phase of the superfluid order parameter; and the precession frequency plays the role of chemical potential, $\mu = \omega$. Note that for the equilibrium planar ferromagnet, which also can be described in terms of the ODLRO, Eq.(12) does not contain the chemical potential ω (see Appendix H); as a result this analogy with magnon Bose condensation^{12,9} (see also²³) becomes too far distant.

The precessing angle β is typically large in HPD. The profile of the spin-orbit energy is such that at $\mu > \omega_L$ (i.e. at $\omega > \omega_L$) the equilibrium condensate corresponds to precession at fixed tipping angle (see Appendix A):

$$\cos \beta \approx -\frac{1}{4}, \quad (13)$$

and thus with fixed condensate density:

$$n_M(\mu = \omega_L + 0) = |\Psi_{\mu=\omega_L+0}|^2 = \frac{5S}{4\hbar}. \quad (14)$$

2.5 Spin supercurrent

The superfluid mass current carried by magnons is the linear momentum of the Bose condensate (see Appendix D):

$$\mathbf{P} = (S - S_z)\nabla\alpha = n_M\hbar\nabla\alpha. \quad (15)$$

Here we used the fact that $S - S_z$ and α are canonically conjugated variables. This superfluid mass current is accompanied by the superfluid current of spins transferred by the magnon condensate. It is determined by the spin to mass ratio

for the magnon, and because the magnon mass is anisotropic, the spin current transferred by the coherent spin precession is anisotropic too:

$$J_z = -\frac{\hbar^2}{m_M^{\parallel}(\beta)} n_M(\beta) \nabla_z \alpha, \quad (16)$$

$$\mathbf{J}_{\perp} = -\frac{\hbar^2}{m_M^{\perp}(\beta)} n_M(\beta) \nabla_{\perp} \alpha. \quad (17)$$

This superfluid current of spins is one more representative of superfluid currents known or discussed in other systems, such as the superfluid current of mass and atoms in superfluid ^4He ; superfluid current of electric charge in superconductors; superfluid current of hypercharge in Standard Model; superfluid baryonic current and current of chiral charge in quark matter; etc.

This superfluidity is very similar to superfluidity of the A_1 phase of ^3He where only one spin component is superfluid²⁴: as a result the superfluid mass current is accompanied by the superfluid spin current.

The anisotropy of the current in Eqs. (16-17) is an important modification of the conventional Bose condensation. This effect is absent in the atomic Bose condensates.

2.6 Two-domain structure of precession

The distinguishing property of the Bose condensate of magnons in $^3\text{He-B}$ is that quasi-equilibrium precession has a fixed density of Bose condensate in Eq.(14). Since the density of magnons in the condensate cannot relax continuously, the decay of the condensate can only occur via the decreasing volume of the condensate.

This results in the formation of two-domain precession: the domain with the Bose condensate (HPD) is separated by a phase boundary from the domain with static equilibrium magnetization (non-precessing domain, or NPD). The two-domain structure spontaneously emerges after the magnetization is deflected by pulsed NMR, and thus magnons are pumped into the system (Fig. 1(a)). If this happens in an applied gradient of magnetic field, the magnons are condensed and collected in the region of the sample, where $\mu \equiv \omega > \omega_L(z)$ (Fig. 1(b)). They form the HPD there. This process is fully analogous to the separation of gas and liquid in the gravitational field: the role of the gravitational field is played by $\nabla \omega_L$.

In the absence of the rf field, i.e. without continuous pumping, the precessing domain (HPD) remains in the fully coherent Bose condensate state, while the phase boundary between HPD and NPD slowly moves up so that the volume of the Bose condensate gradually decreases (Fig. 1(c)). The frequency ω of spontaneous coherence as well as the phase of precession remain homogeneous across the whole Bose condensate domain, but the magnitude of the frequency changes with time. The latter is determined by the Larmor frequency at the position of the phase boundary between HPD and NPD, $\mu \equiv \omega = \omega_L(z_0)$; in other words at the phase boundary the chemical potential of magnons corresponds to the onset of condensation.

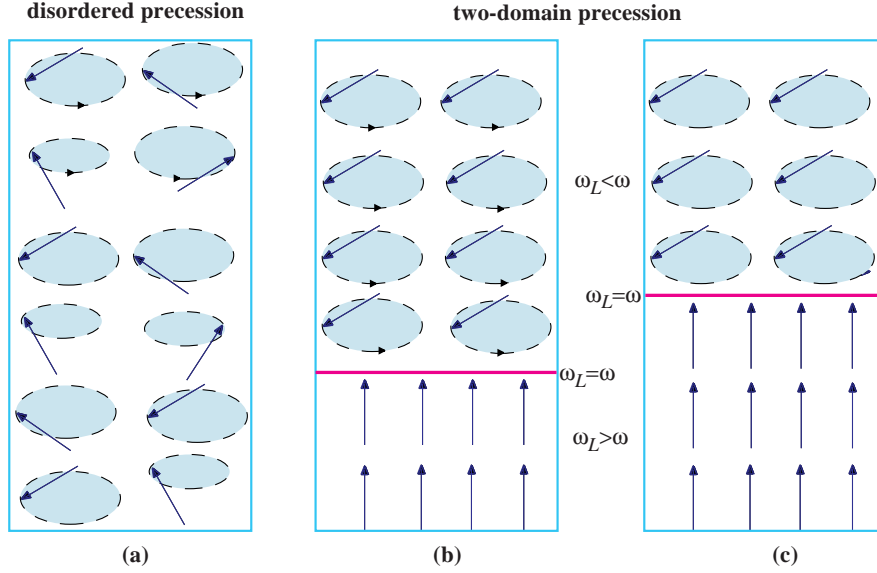


Fig. 1 (a) Disordered precession after pumping of magnons spontaneously evolves into (b) two domains: Homogeneously Precessing Domain (HPD) with the Bose condensate of magnons, and the domain with static magnetization and no magnons (NPD). (c) The Bose condensate decays due to non-conservation of the number of magnons. However, phase coherence is not violated, and even the density of the Bose condensate n_M does not change. The relaxation occurs via gradual decrease of the volume of the Bose condensate.

3 Discussion

3.1 Observed superfluid properties of magnon Bose condensate

As distinct from the conventional Larmor precession, the phase coherent precession of magnetization in $^3\text{He-B}$ has all the properties of the coherent Bose condensate of magnons. The main spin-superfluid properties of HPD have been verified already in early experiments 20 years ago^{1,2,3,4,5,6,7}. These include spin supercurrent which transports the magnetization (analog of the mass current in conventional superfluids); spin current Josephson effect and phase-slip processes at the critical current. Later on a spin current vortex has been observed²⁵ – a topological defect which is the analog of a quantized vortex in superfluids and of an Abrikosov vortex in superconductors (see Appendix D).

The Goldstone modes of the two-domain structure of the Larmor precession have been also observed including the “sound waves” of the magnon condensate – phonos⁵ (see Appendix E) and ‘gravity’ waves - surface waves at the interface between HPD and NPD²⁶.

3.2 Exploiting Bose condensate of magnons

The Bose condensation of magnons in superfluid $^3\text{He-B}$ has many practical applications.

In Helsinki, owing to the extreme sensitivity of the Bose condensate to textural inhomogeneity, the phenomenon of Bose condensation has been applied to studies of supercurrents and topological defects in $^3\text{He-B}$. The measurement technique was called HPD spectroscopy^{27,28}. In particular, HPD spectroscopy provided direct experimental evidence for broken axial symmetry in the core of a particular quantized vortex in $^3\text{He-B}$. Vortices with broken symmetry in the core are condensed matter analogs of the Witten cosmic strings, where the additional $U(1)$ symmetry is broken inside the string core (the so-called superconducting cosmic strings²⁹). The Goldstone mode of the vortex core resulting from the spontaneous violation of rotational $U(1)$ symmetry in the core has been observed³⁰. The so-called spin-mass vortex, which is a combined defect serving as the termination line of the topological soliton wall, has also been observed and studied using HPD spectroscopy³¹.

In Moscow³², Grenoble^{33,34} and Tokyo^{35,36,37}, HPD spectroscopy proved to be extremely useful for the investigation of the superfluid order parameter in a novel system – ^3He confined in aerogel.

There are a lot of new physical phenomena related to the Bose condensation, which have been observed after the discovery. Other coherently precessing spin states have been observed in $^3\text{He-B}$ (see review paper²¹ and Ref.³⁴) and also in $^3\text{He-A}$ ³⁶. These include in particular the compact objects with finite number of the Bose condensed magnons (see Appendix I). At small number N of the pumped magnons, the system is similar to the Bose condensate of the ultracold atoms in harmonic traps, while at larger N the analog of Q -ball in particle physics develops³⁸.

The important property of the condensation of quasiparticles is that the BEC is the time dependent process. That is why it may experience instabilities which do not occur in the equilibrium condensates of stable particles. In 1989 it was found that the original magnon condensate – HPD state – loses its stability below about $0.4 T_c$ ³⁹ and experiences catastrophic relaxation. This phenomenon was left unexplained for a long time and only recently the reason was established: in the low-temperature regime, where dissipation becomes sufficiently small, a Suhl instability in the form of spin wave radiation destroys the homogeneous precession⁴⁰. However, the magnon BEC in harmonic traps and Q -balls are not destroyed.

In conclusion, the Homogeneously Precessing Domain discovered about 20 years ago in superfluid $^3\text{He-B}$ represented the first example of a Bose condensate found in nature (if one does not take into account the strongly interacting superfluid liquid ^4He with its tiny 7% fraction of the Bose condensed atoms).

4 Appendix A. Ginzburg-Landau energy

In $^3\text{He-B}$ the energy of spin-orbit interaction is

$$F_{\text{so}}(\beta) = \frac{8}{15} \chi \Omega_L^2 \left(\cos \beta + \frac{1}{4} \right)^2, \quad \text{when } \cos \beta < -\frac{1}{4}, \quad (18)$$

$$E_{\text{so}}(\beta) = 0 \quad , \quad \text{when } \cos\beta > -\frac{1}{4} . \quad (19)$$

Here Ω_L is the so-called Leggett frequency; in typical NMR experiments $\Omega_L^2 \ll \omega_L^2$, i.e. the spin-orbit interaction is small compared to Zeeman energy. This leads to the following Ginzburg-Landau potential²²

$$F_{\text{so}}(|\Psi|) = \frac{8}{15} \chi \Omega_L^2 \left(\frac{|\Psi|^2}{S} - \frac{5}{4} \right)^2 \Theta \left(\frac{|\Psi|^2}{S} - \frac{5}{4} \right) , \quad (20)$$

where $\Theta(x)$ is Heaviside step function. The total Ginzburg-Landau energy functional is

$$F_{\text{GL}} = \frac{1}{2} (m(|\Psi|))_{ij}^{-1} \nabla_i \Psi^* \nabla_j \Psi + (\omega_L(\mathbf{r}) - \omega) + F_{\text{so}}(|\Psi|) , \quad (21)$$

where $m_{ij}(|\Psi|)$ is the anisotropic mass in the spectrum of magnons, see below Sec. 5; the local Larmor frequency $\omega_L(\mathbf{r})$ plays the role of the external potential acting on magnons; and the global precession frequency ω plays the role of the magnon chemical potential.

The precession frequency is shifted from the Larmor value when $\cos\beta < -1/4$:

$$\mu \equiv \omega = \omega_L + \frac{4}{15} \frac{\Omega_L^2}{\omega_L} (1 + 4 \cos\beta) > \omega_L . \quad (22)$$

The Bose condensate starts with the tipping angle equal to the so-called Leggett angle, $\cos\beta = -1/4$.

5 Appendix B. Magnon spectrum

The spectrum of magnons in the limit of small spin-orbit interaction is

$$\omega(k) = \omega_L + \frac{\hbar k_z^2}{2m_M^{\parallel}(\beta)} + \frac{\hbar k_{\perp}^2}{2m_M^{\perp}(\beta)} , \quad (23)$$

where the longitudinal and transverse masses depend on the tilting angle. For superfluid ³He-B one has the following dependence:

$$\frac{1}{m_M^{\parallel}(\beta)} = 2 \frac{c_{\parallel}^2 \cos\beta + c_{\perp}^2 (1 - \cos\beta)}{\hbar \omega_L} ,$$

$$\frac{1}{m_M^{\perp}(\beta)} = \frac{c_{\parallel}^2 (1 + \cos\beta) + c_{\perp}^2 (1 - \cos\beta)}{\hbar \omega_L} ,$$

where the parameters c_{\parallel} and c_{\perp} are on the order of the Fermi velocity v_F . In the simplified cases $c_{\parallel} = c_{\perp} \equiv c$, when one neglects the spin-wave anisotropy (or in the limit of small tilting angle), the magnon spectrum in the limit of small spin-orbit interaction is

$$\omega(k) = \omega_L + \frac{\hbar k^2}{2m_M} , \quad (24)$$

where the isotropic magnon mass is:

$$m_M = \frac{\hbar\omega_L}{2c^2}. \quad (25)$$

Since $c \sim v_F$, the relative magnitude of the magnon mass compared to the bare mass m of the ${}^3\text{He}$ atom is

$$\frac{m_M}{m} \sim \frac{\hbar\omega_L}{E_F}, \quad (26)$$

where the Fermi energy $E_F \sim mv_F^2 \sim p_F^2/m$.

The spectrum (24) is valid when $kc \ll \omega_L$, however the typical temperature T of HPD is $0.3T_c$ which is an order of magnitude larger than the magnon gap $\hbar\omega_L \sim 50 \mu\text{K}$ at $\omega_L \sim 1\text{MHz}$. That is why one needs the spectrum in the broader range of k :

$$\omega(k) = \pm \frac{\omega_L}{2} + \sqrt{\frac{\omega_L^2}{4} + k^2c^2}, \quad (27)$$

where the sign $+$ corresponds to magnons under discussion. Since $T \gg \hbar\omega_L$ thermal magnons are spin waves with linear spectrum $\omega(k) = ck$, with characteristic momenta $k_T \sim T/\hbar c$. The density of thermal magnons is $n_T \sim k_T^3$.

The density of the condensed of magnons is small when compared to the density of atoms $n = p_F^3/3\pi^2\hbar^3$ in ${}^3\text{He}$ liquid

$$\frac{n_M}{n} \sim \frac{\hbar\omega_L}{E_F} \ll 1. \quad (28)$$

But it is large when compared to the density of thermal magnons:

$$\frac{n_M}{n_T} \sim \frac{\hbar\omega_L}{T} \frac{E_F^2}{T^2} \gg 1, \quad (29)$$

6 Appendix C. Transition temperature

At first glance, the temperature at which condensation starts can be estimated as the temperature at which n_M and n_T are comparable. This gives

$$T_{\text{BEC2}} \sim (\hbar\omega_L E_F^2)^{1/3}, \quad (30)$$

This temperature is much smaller than the estimate in Eq.(10) which comes from the low-frequency part of the spectrum, but still is much bigger than T_c .

However, since the gap ω_L in magnon spectrum is small, the condensation may occur even if the number density of the condensed magnons $n_M \ll n_T$ (see also Refs. ^{15,19}). The number of extra magnons which can be absorbed by thermal distribution is the difference of the distribution function at $\mu = 0$ and $\mu \neq 0$. Since $\mu \ll T$, it is determined by low energy Rayleigh-Jeans part of the spectrum:

$$n_{\text{extra}} = \sum_{\mathbf{k}} \left(\frac{T}{\varepsilon - \mu} - \frac{T}{\varepsilon} \right), \quad (31)$$

Maximum takes place when $\mu = \omega_L$, which gives the dependence of transition temperature on the number of pumped magnons

$$\frac{n_M}{T_{\text{BEC3}}} = \frac{1}{4\pi} \int dk k^2 \left(\frac{\omega_L}{k^2 c^2} - \frac{\omega_L}{\omega_L^2 + k^2 c^2} \right) = \frac{\omega_L^2}{4c^3}. \quad (32)$$

This gives the transition temperature

$$T_{\text{BEC3}} = \frac{4n_M c^3}{\omega_L^2} \sim \frac{E_F^2}{\omega_L}, \quad (33)$$

which is much bigger than the estimations (30) and (10).

In any case, at the typical temperatures of superfluid ^3He of order $T \sim 10^{-3} E_F$ the Bose condensation is complete. The hierarchy of temperatures in magnon BEC is thus

$$\hbar\omega_L \ll T \ll T_{\text{BEC}}. \quad (34)$$

Bose condensation of magnons in $^3\text{He-B}$ is similar to the Bose condensation of ultrarelativistic particles with spectrum $E(p) = \sqrt{M^2 c^4 + c^2 p^2}$ in the regime when

$$M c^2 \ll T \ll T_{\text{BEC}}. \quad (35)$$

For the Bose gas in laser traps, the hierarchy of temperatures is $\hbar\omega_h \ll T < T_{\text{BEC}}$, where ω_h is the frequency in the harmonic trap⁴¹.

7 Appendix D. Superflow

In the simple case of isotropic mass the kinetic energy of superflow of magnon BEC in the London limit is

$$E_{\text{kin}} = \frac{1}{2} \rho_{sM} \mathbf{v}_{sM}^2, \quad \mathbf{v}_{sM} = \frac{\hbar}{m_M} \nabla \alpha, \quad \rho_{sM} = n_M m_M. \quad (36)$$

Here \mathbf{v}_{sM} and ρ_{sM} are superfluid velocity and density of magnon superfluidity. Note that the total number of magnons enters ρ_{sM} , since the temperature is low, and the number of thermal magnons is negligibly small. In the Ginzburg-Landau regime this has the form:

$$E_{\text{kin}} = \frac{\hbar^2}{2m_M} |\nabla \Psi|^2, \quad (37)$$

and the total GL functional is

$$E_{\text{GL}} = \frac{\hbar^2}{2m_M} |\nabla \Psi|^2 + (\omega_L - \mu) |\Psi|^2 + F_{\text{so}}(\Psi), \quad (38)$$

The mass supercurrent generated by magnons is

$$\mathbf{P} = \rho_{sM} \mathbf{v}_{sM} = \hbar n_M \nabla \alpha, \quad (39)$$

which gives Eq.(15).

Circulation quantum is

$$\kappa_M = \oint d\mathbf{r} \cdot \mathbf{v}_{sM} = \frac{2\pi\hbar}{m_M}. \quad (40)$$

This demonstrates that the observed spin vortex²⁵ with nonzero winding of α has also circulation of the mass current. This is similar to the A_1 phase of ^3He with the superfluidity of only one spin component: the superfluid mass current is accompanied by the superfluid spin current.

8 Appendix E. Phonons in magnon superfluid and symmetry breaking field

The speed of sound in magnon superfluid is determined by compressibility of magnons gas, which is non-zero due to dipole interaction. Applying Eq.(38) in the HPD region, i.e. in the region where $\cos\beta < -1/4$, and using the isotropic spin wave approximation $c_{\parallel} = c_{\perp}$ (for anisotropic spin wave velocity see e.g. Ref.⁴²) one obtains the sound with velocity:

$$c_s^2 = \frac{1}{m_M} \frac{dP}{dn_M} = \frac{n_M}{m_M} \frac{d\mu}{dn_M} = \frac{n_M}{m_M} \frac{d^2 E_{so}}{dn_M^2}. \quad (41)$$

For $\cos\beta$ close to $-1/4$ the speed of sound is

$$c_s^2 = \frac{8}{3} \frac{\Omega_L^2}{\omega_L^2} c^2. \quad (42)$$

This sound observed in Ref.⁵ is the Goldstone mode of the magnon Bose condensation.

The important property of magnon BEC is that the Goldstone boson (phonon) acquires mass (gap) due to the transverse RF field \mathbf{H}_{RF} . The latter plays the role of the symmetry breaking field, since it violates the $U(1)$ symmetry of precession⁴². As a result, the extra term in the Ginzburg-Landau energy, $F_{\text{RF}} = -\gamma\mathbf{H}_{\text{RF}} \cdot \mathbf{S}$, induced by \mathbf{H}_{RF} depends explicitly on the phase of precession α with respect to the direction of the RF-field in rotating frame. For $\cos\beta = -1/4$ one has

$$F_{\text{RF}} = -\gamma H_{\text{RF}} S_{\perp} \cos\alpha \approx -\frac{\sqrt{15}}{4} \left(1 - \frac{\alpha^2}{2}\right) \gamma H_{\text{RF}} S. \quad (43)$$

This term adds the mass (gap) to the phonon spectrum:

$$\omega_s^2(k) = c_s^2 k^2 + m_s^2, \quad m_s^2 = \frac{4}{\sqrt{15}} \gamma H_{\text{RF}} \frac{\Omega_L^2}{\omega_L}. \quad (44)$$

The gap m_s of the Goldstone mode induced by the symmetry breaking field has been measured in Refs.^{43,44}.

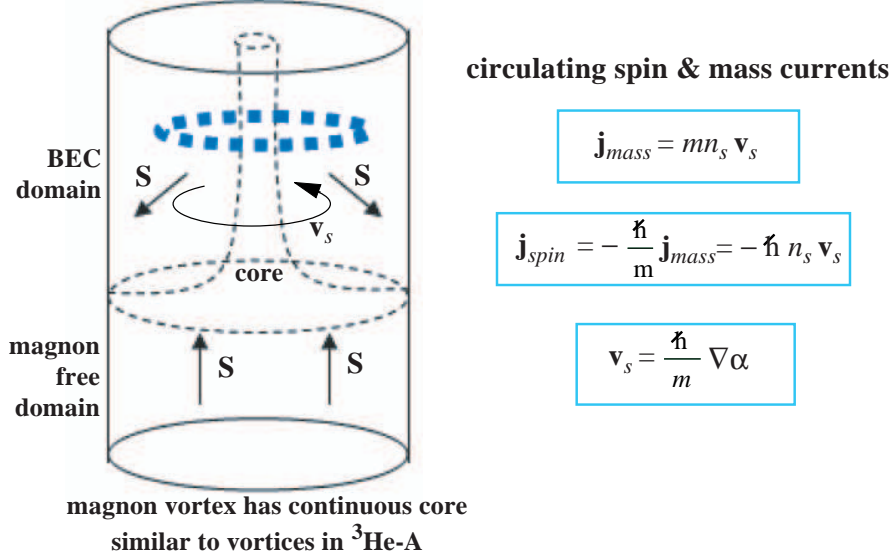


Fig. 2 Spin-mass vortex in magnon BEC. The spin current around the vortex core is accompanied by mass current. According to Eq.(46) the size of the vortex core diverges when the HPD domain boundary is approached where the local Larmor frequency $\omega_L = \omega$.

9 Appendix F. Critical velocities and vortex core

The speed of sound in magnon gas determines the Landau critical velocity of the counterflow at which phonons are created:

$$v_L = c_s . \quad (45)$$

For conventional condensates this suggests that the coherence length and the size of the vortex core should be:

$$\frac{\hbar}{m_M c_s} \sim \frac{c}{\Omega_L} \sim \xi_D . \quad (46)$$

However, for magnons BEC in $^3\text{He-B}$ this gives only the lower bound on the core size. The core is larger due to specific profile of the Ginzburg-Landau (dipole) energy in Eq.(20) which is strictly zero for $\cos \beta > -1/4$. This leads to the special topological properties of coherent precession (see Ref.⁴⁵). As a result the spin vortex created and observed in Ref.²⁵ has a continuous core with broken symmetry, similar to vortices in superfluid $^3\text{He-A}$ ⁴⁶. The size of the continuous core is determined by the proper coherence length⁴⁷ which can be found from the competition between the first two terms in Eq.(38):

$$r_{\text{core}} \sim \frac{\hbar}{\sqrt{m_M(\mu - \omega_L)}} \sim \frac{c}{\sqrt{\omega_L(\omega - \omega_L)}} . \quad (47)$$

This coherence length determines also the critical velocity for creation of vortices:

$$v_c \sim \frac{\hbar}{m_M r_{\text{core}}} . \quad (48)$$

For large tipping angles of precession the symmetry of the vortex core is restored: the vortex becomes singular with the core radius $r_{\text{core}} \sim \xi_D^{48}$.

10 Appendix G. BEC in YIG

Magnons in yttrium-iron garnet (YIG) films have the quasi 2D spectrum:^{15,19}

$$\omega_n(k_x, k_y) = \Delta_n + \frac{k_y^2}{2m_y} + \frac{(k_x - k_0)^2}{2m_x} , \quad (49)$$

where magnetic field is along x ; the gap in the lowest branch $\Delta_0 = 2.1$ GHz \equiv 101 mK at $H = 700$ Oe¹⁵ and $\Delta_0 = 2.9$ GHz at $H = 1000$ Oe¹⁹; the position of the minimum $k_0 = 5 \cdot 10^4$ 1/cm¹⁵; the anisotropic magnon mass can be probably estimated as $m_x \sim k_0^2/\Delta$ with m_y being somewhat bigger, both are of order of electron mass.

If one neglects the contribution of the higher levels and consider the 2D gas, the Eq.(31) becomes

$$n_{\text{extra}} = \frac{T}{2\pi\hbar} \sqrt{m_x m_y} \ln \frac{\Delta_0}{\Delta_0 - \mu} , \quad (50)$$

In 2D, all extra magnons can be absorbed by thermal distribution at any temperature without formation of Bose condensate. The larger is the number n_M of the pumped magnons the closer is μ to Δ_0 , but μ never crosses Δ_0 . At large n_M the chemical potential exponentially approaches Δ_0 from below and the width of the distribution becomes exponentially narrow:

$$\frac{(\delta k_y)^2}{m_y \Delta_0} \sim \frac{(\delta k_x)^2}{m_x \Delta_0} \sim \frac{\Delta_0 - \mu}{\Delta_0} \sim \exp\left(-\frac{2\pi\hbar n_M}{T\sqrt{m_x m_y}}\right) . \quad (51)$$

If one uses the 2D number density $n_M = \delta N d$ with the film thickness $d = 5$ μm and 3D number density $\delta N \sim 5 \cdot 10^{18}$ cm⁻³, one obtains that at room temperature the exponent is

$$\frac{2\pi\hbar n_M}{T\sqrt{m_x m_y}} \sim \frac{2\pi\Delta_0}{T} \frac{\delta N d}{10k_0^2} \sim 10^2 . \quad (52)$$

If this estimation is correct, the peak should be extremely narrow, so that all extra magnons are concentrated at the lowest level of the discrete spectrum. However, there are other contributions to the width of the peak due to: finite resolution of spectrometer, magnon interaction, finite life time of magnons and the influence of the higher discrete levels $n \neq 0$.

In any case, the process of the concentration of extra magnons in the states very close to the lowest energy is the signature of the BEC of magnons. The main property of the room temperature BEC in YIG is that the transition temperature

T_c is only slightly higher than temperature, $T_c - T \ll T$; as a result the number of condensed magnons is small compared to the number of thermal magnons: $n_M \ll n_T$. Situation with magnon BEC in ${}^3\text{He}$ is the opposite, one has $T \ll T_c$ and thus $n_M \gg n_T$.

11 Appendix H. Magnon BEC vs planar ferromagnet

Coherently precessing state HPD state in ${}^3\text{He-B}$ has

$$S_x + iS_y = S_{\perp} e^{i\omega t + i\alpha} . \quad (53)$$

The coherent state in YIG has

$$S_x + iS_y = S_{\perp} \cos(k_0 x) e^{i\omega t + i\alpha} . \quad (54)$$

For equilibrium planar ferromagnet one has^{23,12}

$$S_x + iS_y = S_{\perp} e^{i\alpha} . \quad (55)$$

This means that the equilibrium planar ferromagnet can be also described in terms of the ODLRO.

Magnons were originally determined as second quantized modes in the background of stationary state with magnetization along z axis. Both the static state in Eq.(55) and precessing states (53) and (54) can be interpreted as BEC of these original magnons. On the other hand, the stationary and precessing states can be presented as new vacuum states, the time independent and the time dependent vacua respectively. The excitations – phonons – are the second quantized modes in the background of a new vacuum. What is the principle difference between the stationary vacuum of planar ferromagnet and the time dependent vacuum of coherent precession?

The major point which distinguishes the HPD state (53) in ${}^3\text{He-B}$ and the coherent precession (54) in YIG from the equilibrium magnetic states is the conservation (or quasi-conservation) of the $U(1)$ charge Q . The charge Q is played by the spin projection S_z in magnetic materials (or the related number N of magnons) and by number N of atoms in atomic BEC. This conservation gives rise to the chemical potential $\mu = dE/dN$, which is the precession frequency ω in magnetic systems. On the contrary, the static state in Eq.(55) does not contain the chemical potential ω , i.e. the conservation is not in the origin of formation of the static equilibrium state.

The spin-orbit interaction violates the conservation of S_z , as a result the life time of magnons is finite. For the precessing states (53) and (54) this leads to the finite life time of the coherent precession. To support the steady state of precession the pumping of spin and energy is required. On the contrary, the spin-orbit interaction does not destroy the long-range magnetic order in the static state (55): this is fully equilibrium state which does not decay and thus does not require pumping: the life time of static state is macroscopically large and thus by many orders of magnitude exceeds the magnon relaxation time. That is why a planar ferromagnet (55) is just one more equilibrium state of quantum vacuum, in addition to the easy axis ferromagnetic state, rather than the magnon condensate.

The property of (quasi)conservation of the $U(1)$ charge Q distinguishes the coherent precession from the other coherent phenomena, such as optical lasers and standing waves.

12 Appendix I. Finite-size BEC & Q -ball

When $\cos \beta > -1/4$ ($\beta < 104^\circ$), the spin-orbit interaction $F_{\text{so}}(\Psi)$ becomes nonzero at finite polar angle β_L of vector \mathbf{L} of $^3\text{He-B}$ orbital angular momentum:

$$F_{\text{so}}(\Psi) = \chi \Omega_L^2 \left[\frac{4 \sin^2(\beta_L/2)}{5S} |\Psi|^2 - \frac{\sin^4(\beta_L/2)}{S^2} |\Psi|^4 \right], \quad (56)$$

As a result the texture of vector \mathbf{L} forms the potential well for magnons.

Four regimes of magnon condensation are possible in the potential well, which correspond to four successive ranges of the $U(1)$ charge Q (magnon number N). (i) At the smallest N the interaction can be neglected and the non-interacting magnons occupy the lowest energy state in the potential well. (ii) With increasing N the Thomas-Fermi regime of interacting magnons is reached. (iii) When the number of magnons is sufficiently large, they start to modify the potential well; this is the regime of the so-called Q -ball³⁸. (iv) Finally when the size of the Q -ball reaches the dimension of the experimental cell the homogeneous BEC is formed – the HPD.

The first two regimes are similar to what occurs in atomic BEC in laser traps, though not identical. The difference comes from the 4-th order term in the GL energy (56) which demonstrates that the attractive interaction between magnons is determined by the texture

$$F_{\text{so}}(\Psi) = U(r)|\Psi|^2 + V(r)|\Psi|^4, \quad (57)$$

In the simplest case of the spherically symmetric harmonic trap one has

$$U(r) = m_M \omega_h^2 r^2, \quad V(r) = -\mu' \left(\frac{\omega_h r}{c_s} \right)^4, \quad (58)$$

where ω_h is the harmonic oscillator frequency; the magnon interaction is normalized to its magnitude $\mu' = d\mu/dn_M$ in the HPD state and to the speed of sound c_s , also in the HPD state.

The first two regimes can be qualitatively described using simple dimensional analysis. Let r_N is the dimension of magnon gas as a function of the magnon number N . Taking into account that $N \sim |\Psi|^2 r_N^3$, one estimates the GL energy (38) of the condensate as:

$$F \sim N \left(\omega_L + \frac{3}{4} \omega_h \left(\frac{r_h^2}{r_N^2} + \frac{r_N^2}{r_h^2} \right) - \gamma N r_N \right). \quad (59)$$

Here $r_h = (m_M \omega_h)^{-1/2}$ is the harmonic oscillator length; the prefactor 3/4 is introduced to match the oscillator frequency after minimization over r_N in the linear regime; and $\gamma = \mu' (\omega_h/c_s)^4$. Minimization at fixed magnon number N gives two regimes.

(i) In the regime linear in N (the regime of spin-waves) one obtains the N -independent radius $r_N = r_h$; and the Bose condensation occurs at the lowest energy level which corresponds to the precession with frequency (chemical potential)

$$\omega - \omega_L \approx \frac{3}{2}\omega_h, \quad N \ll N_1 = \frac{\omega_h}{r_h\gamma}. \quad (60)$$

(ii) At larger $N \gg N_1$ one obtains the analog of the Thomas-Fermi droplet whose size and precession frequency depend on N :

$$r_N \sim r_h \frac{N}{N_1}, \quad \omega - \omega_L \sim -\omega_h \frac{N^2}{N_1^2}, \quad N \gg N_1. \quad (61)$$

For comparison, the atomic BEC in the nonlinear regime, which can be obtained by the same procedure, is characterized by⁴¹

$$r_N \sim r_h \left(\frac{N}{N_1}\right)^{1/5}, \quad \mu \sim \omega_h \left(\frac{N}{N_1}\right)^{2/5}, \quad N \gg N_1, \quad (62)$$

where $N_1 = r_h/a$ with a being the scattering length.

(iii) The regime of Q -ball emerges when the density of magnons in center of the droplet is such that β is not small, and the spin-orbit interaction starts to modify the potential well. This regime develops when N approaches the characteristic value N_2 :

$$N_2 = N_1 \frac{c_s}{\omega_h r_h} \sim \frac{c_s}{r_h^2 \gamma} \sim N_1 \sqrt{\frac{m_M c_s^2}{\omega_h}}. \quad (63)$$

(iv) Finally, the HPD emerges when the size of the droplet reaches the size L of the cell, and the magnon number N reaches the maximum value $N_{\max} \sim n_M L^3$, where n_M is magnon density in HPD.

A typical texture in the vessel is determined by the vessel geometry and thus by dimension L of the cell, $\beta_L \sim r/L$. In such cases, the corresponding parameters are

$$\omega_h \sim \frac{c_s}{L}, \quad r_h \sim \sqrt{L\xi_D}, \quad N_1 \sim N_{\max} \left(\frac{\xi_D}{L}\right)^{1/2}, \quad N_2 \sim N_{\max}. \quad (64)$$

Here $\xi_D = c/\Omega_L \sim 10^{-3}$ cm is the dipole length. Since $N_2 \sim N_{\max}$, the Q -ball regime develops at $N \lesssim N_{\max}$, and then Q -ball transforms to HPD when N approaches N_{\max} . In the applied external gradient of magnetic field the two-domain state in Fig. 1 emerges earlier.

One may expect a similar finite size BEC of magnons in rotating $^3\text{He-A}$, where the trap for magnons is provided by the core of individual continuous 4π vortex⁴⁶. Applying gradient of magnetic field one may study individual vortices by the magnon BEC tomography.

Acknowledgements I am grateful to Yu.M. Bunkov, S. Demokritov, V.V. Dmitriev, V.B. Eltsov, I.A. Fomin, M. Krusius and V.S. L'vov for illuminating discussions. This work was supported in part by ESF COSLAB Programme and by the Russian Foundation for Basic Research (grant 06-02-16002-a).

References

1. A.S. Borovik-Romanov, Yu.M. Bunkov, V.V. Dmitriev, Yu. M. Mukharskiy, Long Lived Induction Decay Signal Investigations in ^3He , JETP Lett. **40**, 1033 (1984)
2. I.A. Fomin, Long-lived induction signal and spatially nonuniform spin precession in $^3\text{He-B}$, JETP Lett. **40**, 1037 (1984)
3. A.S. Borovik-Romanov, Yu.M. Bunkov, V.V. Dmitriev, Yu. M. Mukharskiy, K. Flahbart, Stratification of $^3\text{He-B}$ Spin Precession on Two Magnetic Domains, Sov. Phys. JETP **61**, 1199 (1985)
4. I.A. Fomin. Separation of magnetization precession in $^3\text{He-B}$ into two magnetic domains. Theory, Sov. Phys. JETP **61**, 1207 (1985)
5. Yu.M. Bunkov, V.V. Dmitriev, Yu.M. Mukharskiy, Twist Oscillations of Homogeneous Precession Domain in $^3\text{He-B}$, JETP Lett. **43**, 168 (1986)
6. A.S. Borovik-Romanov, Yu.M. Bunkov, V.V. Dmitriev, Yu.M. Mukharskiy, Phase Slipage Observations of Spin Supercurrent in $^3\text{He-B}$, JETP Lett. **45**, 124 (1987)
7. A.S. Borovik-Romanov, Yu.M. Bunkov, A. de Waard, V.V. Dmitriev, V. Makrotsieva, Yu.M. Mukharskiy, D.A. Sergatskov, Observation of a Spin Supercurrent Analog of the Josephson Effect, JETP Lett. **47**, 478 (1988)
8. T. Radu, H. Wilhelm, V. Yushankhai, D. Kovrizhin, R. Coldea, Z. Tylczynski, T. Lühmann, F. Steglich, Radu et al. Reply, Phys. Rev. Lett. **98**, 039702 (2007)
9. T. Giamarchi, Ch. Rüegg, O. Tchernyshyov, Bose-Einstein condensation in magnetic insulators, Nature Physics **4**, 198–204 (2008); arXiv:0712.2250
10. D.L. Mills, A comment on the letter by T. Radu et al., Phys. Rev. Lett. **98**, 039701 (2007)
11. W. Kohn, D. Sherrington, Two Kinds of Bosons and Bose Condensates, Rev. Mod. Phys. **42**, 1–11 (1970)
12. T. Nikuni, M. Oshikawa, A. Oosawa, H. Tanaka, Bose-Einstein Condensation of Dilute Magnons in TiCuCl_3 , Phys. Rev. Lett. **84**, 5868–5871 (2000)
13. L.D. Landau and E.M. Lifshitz, *Fluid Mechanics*, Pergamon, Oxford (1959)
14. V.E. Zakharov, S.V. Nazarenko, Dynamics of the Bose-Einstein condensation, Physica **D 201**, 203–211 (2005)
15. S.O. Demokritov, V.E. Demidov, O. Dzyapko, G.A. Melkov, A.A. Serga, B. Hillebrands, A.N. Slavin, Bose-Einstein condensation of quasi-equilibrium magnons at room temperature under pumping, Nature **443**, 430–433 (2006)
16. J. Kasprzak, M. Richard, S. Kundermann, A. Baas, P. Jeambrun, J.M.J. Keeling, F.M. Marchetti, M.H. Szymaska, R. Andre, J.L. Staehli, V. Savona, P.B. Littlewood, B. Deveaud, Le Si Dang, Bose-Einstein condensation of exciton polaritons, Nature **443**, 409–414 (2006)
17. D. Snoke, Coherent questions, Nature **443**, 403–404 (2006)
18. Yu.D. Kalafati and V.L. Safonov, Possibility of Bose condensation of magnons excited by incoherent pump, JETP Lett. **50**, 149–151 (1989)
19. V.E. Demidov, O. Dzyapko, S.O. Demokritov, G.A. Melkov and A.N. Slavin, Observation of Spontaneous Coherence in Bose-Einstein Condensate of Magnons, Phys. Rev. Lett. **100**, 047205 (2008)
20. Yu. Bunkov, Spin Supercurrent, Proceedings ICM2006; cond-mat/0701182

21. Yu.M. Bunkov, G.E. Volovik, Bose-Einstein condensation of magnons in superfluid ^3He , *J. Low Temp. Phys.* **150**, 135–144 (2008); arXiv:0708.0663
22. I.A. Fomin, Spin currents in superfluid ^3He , *Physica B* **169**, 153 (1991)
23. P.C. Hohenberg, in: *Critical Phenomena. Proc. Int. School Phys. “Enrico Fermi”*. Course LI., Acad. Press, NY (1971)
24. D. Vollhardt, P. Wölfle, *The superfluid phases of helium 3*, Taylor and Francis, London (1990)
25. A.S. Borovik-Romanov, Yu.M. Bunkov, V.V. Dmitriev, Yu.M. Mukharskiy, D.A. Sergatskov, Observation of Vortex-like Spin Supercurrent in $^3\text{He-B}$, *Physica B* **165**, 649 (1990)
26. Yu.M. Bunkov, V.V. Dmitriev, Yu.M. Mukharskiy, Low frequency oscillations of the homogeneously precessing domain in $^3\text{He-B}$, *Physica B* **178**, 196 (1992)
27. Yu.M. Bunkov, Principles of HPD NMR spectroscopy of $^3\text{He-B}$, *Physica B* **178**, 187 (1992)
28. J.S. Korhonen, Yu.M. Bunkov, V.V. Dmitriev, Y. Kondo, M. Krusius, Yu.M. Mukharskiy, U. Parts, E.V. Thuneberg, Homogeneous spin precession in rotating vortex-free $^3\text{He-B}$; measurements of the superfluid density anisotropy, *Phys. Rev.* **46**, 13983 (1992)
29. E. Witten, Superconducting strings, *Nucl. Phys.* **B249**, 557–592 (1985)
30. Y. Kondo, J.S. Korhonen, M. Krusius, V.V. Dmitriev, Y. M. Mukharsky, E.B. Sonin, G.E. Volovik, Direct observation of the nonaxisymmetric vortex in superfluid $^3\text{He B}$, *Phys. Rev. Lett.* **67**, 81–84 (1991)
31. Y. Kondo, J.S. Korhonen, M. Krusius, V.V. Dmitriev, E.V. Thuneberg, G.E. Volovik, Combined spin-mass vortex with soliton tail in superfluid $^3\text{He-B}$, *Phys. Rev. Lett.* **68**, 3331–3334 (1992)
32. V.V. Dmitriev, V.V. Zavjalov, D.E. Zmeev, I.V. Kosarev, N. Mulders, Nonlinear NMR in a superfluid B phase of ^3He in aerogel, *JETP Lett.* **76**, 321 (2002); V.V. Dmitriev, V.V. Zavjalov, D. Ye. Zmeev, Measurements of the Leggett frequency in $^3\text{He-B}$ in aerogel, *JETP Lett.* **76**, 499 (2004)
33. Yu.M. Bunkov, E. Collin, H. Godfrin, R. Harakaly, Topological defects and coherent magnetization precession of ^3He in aerogel, *Physica B* **329**, 305 (2003)
34. J. Elbs, Yu. M. Bunkov, E. Collin, H. Godfrin, G. E. Volovik, Strong orientational effect of stretched aerogel on the ^3He order parameter, *Phys. Rev. Lett.* **100**, 215304 (2008)
35. T. Kunimatsu, A. Matsubara, K. Izumina, T. Sato, M. Kubota, T. Takagi, Yu.M. Bunkov, T. Mizusaki, Quantum fluid dynamics of rotating superfluid ^3He in aerogel, *J. Low Temp. Phys.* **150**, 435–444 (2008)
36. T. Sato, T. Kunimatsu, K. Izumina, A. Matsubara, M. Kubota, T. Mizusaki, Yu.M. Bunkov, Observation of coherent precession of magnetization in superfluid $^3\text{He A}$ -phase; arXiv:0804.2994
37. T. Kunimatsu, T. Sato, K. Izumina, A. Matsubara, Y. Sasaki, M. Kubota, O. Ishikawa, T. Mizusaki, Yu.M. Bunkov, The Orientation Effect on Superfluid ^3He in Anisotropic Aerogel, *JETP Lett.* **86**, 216–220 (2007)
38. Yu.M. Bunkov, G.E. Volovik, Magnons condensation into Q -ball in $^3\text{He-B}$, *Phys. Rev. Lett.* **98**, 265302 (2007)

-
39. Yu.M. Bunkov, V.V. Dmitriev, Yu.M. Mukharskiy, J. Nyeki, D.A. Sergatskov, Catastrophic relaxation in $^3\text{He-B}$ at $0.4 T_c$, *Europhys. Lett.* **8**, 645 (1989)
 40. E.V. Surovtsev, I.A. Fomin, Parametric instability of uniform spin precession in superfluid $^3\text{He-B}$, *JETP Lett.* **83**, 410 (2006); Yu.M. Bunkov, V.S. Lvov, G.E. Volovik, Solution of the problem of catastrophic relaxation of homogeneous spin precession in superfluid $^3\text{He-B}$, *JETP Lett.* **83**, 530 (2006); Yu.M. Bunkov, V.S. Lvov, G.E. Volovik, On the problem of catastrophic relaxation in superfluid $^3\text{He-B}$, *JETP Lett.* **84**, 289 (2006)
 41. F. Dalfovo, S. Giorgini, L.P. Pitaevskii, S. Stringari, Theory of Bose-Einstein condensation in trapped gases, *Rev. Mod. Phys.* **71**, 463–512 (1999)
 42. G.E. Volovik, Phonons in magnon superfluid and symmetry breaking field, *Pis'ma ZhETF* **87**, 736–737 (2008); arXiv:0804.3709
 43. V.V. Dmitriev, V.V. Zavjalov, D.Ye. Zmeev, Spatially homogeneous oscillations of homogeneously precessing domain in $^3\text{He-B}$, *J. Low Temp. Phys.* **138**, 765–770 (2005)
 44. M. Človečko, E. Gažo, M. Kupka and P. Skyba, New non-Goldstone collective mode of BEC of magnons in superfluid $^3\text{He-B}$, *Phys. Rev. Lett.* **100**, 155301 (2008)
 45. T.Sh. Misirpashaev and G.E. Volovik, Topology of coherent precession in superfluid $^3\text{He-B}$, *JETP* **75**, 650–665 (1992)
 46. M.M. Salomaa, G.E. Volovik, Quantized vortices in superfluid ^3He , *Rev. Mod. Phys.* **59**, 533–613 (1987)
 47. I.A. Fomin, Critical superfluid spin current in $^3\text{He-B}$, *JETP Lett.* **45**, 106–108 (1987)
 48. E.B. Sonin, Spin-precession vortex and spin-precession supercurrent stability in $^3\text{He-B}$, *JETP Lett.* **88**, (2008); arXiv:0805.1534